Published in final edited form as:
J Orthop Res. 2009 March ; 27(3): 366–373. doi:10.1002/jor.20735.

Acceleration of Spinal Fusion Using Syngeneic and Allogeneic Adult Adipose Derived Stem Cells in a Rat Model

Mandi J. Lopez[1], **Kevin R. McIntosh**[2], **Nakia D. Spencer**[1], **Jade N. Borneman**[2], **Ronald Horswell**[3], **Paul Anderson**[4], **Gang Yu**[3], **Lorrie Gaschen**[1], and **Jeffrey M. Gimble**[3]

[1]Laboratory for Equine and Comparative Orthopedic Research, Department of Veterinary Clinical Sciences, School of Veterinary Medicine, Skip Bertman Drive, Louisiana State University, Baton Rouge, Louisiana 70803

[2]Cognate BioServices, Inc., 1448 S. Rolling Road, Baltimore, Maryland 21227

[3]Stem Cell Laboratory, Pennington Biomedical Research Center, Louisiana State University System, Baton Rouge, Louisiana 70808

[4]Department of Orthopedics & Rehabilitation, University of Wisconsin–Madison, Madison, Wisconsin 53792

Abstract

Posterolateral spinal fusion is the standard treatment for lumbar compression fractures. Adult adipose tissue-derived stem cells (ASCs) promote osteogenesis in vivo and in vitro. The hypothesis tested in this study was that syngeneic and allogeneic ASCs on a biomaterial scaffold composed of tricalcium phosphate and collagen I will accelerate spinal fusion in a rat model. ASCs from male Fischer or ACI rats were loaded onto scaffolds (53,571 cells/mm^3) and cultured in stromal media for 48 h. Male Fisher rats were assigned to 4 cohorts (n = 14/cohort) after bilateral decortication of the L4 and L5 transverse processes: (1) No treatment; (2) scaffold only; (3) scaffold + syngeneic ASCs; or (4) scaffold + allogeneic ASCs. Half of each cohort was harvested 4 or 8 weeks after surgery. Spinal fusion was evaluated with radiographs, microcomputed tomography, and light microscopy. Callus did not form in spines without scaffolds. There were no significant differences in callus formation among scaffold cohorts 4 weeks after surgery. Callus formation was more mature in both ASC cohorts versus scaffold alone 8 weeks after surgery based on microstructure as well as radiographic and microcomputed tomographic evidence of active bone formation. Inflammatory cell infiltrate was significantly lower in both ASC cohorts (syngeneic = 18.3±0.85%; allogeneic = 23.5±2.33%) versus scaffold alone (46.8±11.8%) 4 weeks after surgery. Results of this study support syngeneic and allogeneic ASC acceleration of posterior lumbar spinal fusion in a rat model.

Keywords

adipose; adult stem cells; spine; fusion; rat

Posterolateral intertransverse fusion is frequently used to achieve lumbar intersegmental arthrodesis.[1] Autogenous bone graft harvested from the iliac crest has long been the gold standard for fusion procedures due to its osteoinductive and osteoconductive properties. However, there is significant morbidity associated with the harvest procedure.[2] Allograft bone is routinely used as an alternative to autogenous bone but concerns about immunogenicity and

Correspondence to: Mandi J. Lopez (T: 225-578-9918; F: 225-578-9559; mlopez@vetmed.lsu.edu).

disease transmission surround its use.[3] Additionally, allograft bone has been used successfully in the cervical and lumbar spine, but fusion rates for multilevel cervical and posterior lumbar procedures are much lower.[4] These and other difficulties with bone grafts drive intensive research efforts to develop alternative spinal fusion procedures.

There are more than 185,000 spinal arthrodesis procedures performed in the United States each year.[3] Regardless of the technique used to achieve lumbar fusion for spinal stabilization, fusion rates are variable.[5] In addition, pseudoarthrosis after noninstrumented lumbar intertransverse fusion is as high as 40%.[6] There are anumber of factors inherent to the spine contributing to failure of the fusion process including tensile forces, low parent bone surface, and interference by surrounding musculature.[7] Concomitant patient conditions such as advanced age and osteoporosis as well as corticosteroid, tobacco, and nonsteroidal anti-inflammatory drug use also interfere with successful spinal fusion.[4] Methods to facilitate the process of spinal fusion will significantly improve patient outcome despite potential complicating factors.

Adult bone marrow-derived mesenchymal stem cells (BMSCs) are used widely in tissue engineering.[8] The multipotent differentiation capability and self-regeneration capacity of BMSCs make them strong candidates for tissue regeneration applications.[9] Furthermore, BMSCs display properties of immune privilege allowing them to be transplanted allogeneically without immune rejection.[10,11] The BMSCs are well characterized and enhance fracture repair in both human patients and animal models.[8,5,9,12] Adipose tissue has been described more recently as an abundant source of adult mesenchymal-like stem cells capable of differentiating toward adipogenic, chondrogenic, myogenic, neurogenic, or osteogenic lineages,[8,9,12–18] although there are conflicting reports surrounding the ability of adult adipose derived stem cells (ASCs) to differentiate into neurons.[19] The capacity of ASCs to generate bone both in vivo and in vitro is well established, and recently, human ASCs were shown to accelerate bone formation in a rat calvarial defect model.[8,16–18] The relative ease of harvest and availability of higher numbers of ASCs compared to BMSCs support investigation of ASCs for bone regeneration purposes.[8,9,12–18] In addition, ASCs have recently been reported to exhibit properties of immune privilege suggesting that they can be successfully transplanted from one individual to another.[20,21] The focus of investigations surrounding adult stem cell applications to accelerate spinal fusion has been primarily on BMSCs, and there have been encouraging results for their potential application.[3,22–24] However, equivalent information surrounding the use of ASCs for the same purpose is limited.[15,17] This study was designed to investigate the effects of syngeneic and allogeneic ASCs on a bioabsorbable scaffold in a rat lumbar fusion model to test the hypothesis that both ASC populations would enhance the fusion process compared to scaffold alone or no treatment.

MATERIALS AND METHODS

Experimental Design

This study was performed in accordance with institutional and National Institutes of Health regulations governing the treatment of vertebrate animals. Procedures were initiated after approval by the University Animal Care Committee. ASCs were produced from inguinal adipose tissue derived from Fisher and ACI rats, expanded over four to five passages and cryopreserved in liquid nitrogen until use. Prior to surgery, ASCs were thawed, rinsed, resuspended in media, and loaded onto scaffolds. They were cultured for 48 h prior to application. A total of 56, 10-week-old male Fisher rats weighing 210 ± 2.08 g (mean ± SEM), were used for the spinal fusion aspect of the study. Animals were randomly assigned to four different treatment cohorts after bilateral decortication of the L4 and L5 transverse processes (n = 14/cohort): (1) no treatment; (2) scaffold only; (3) scaffold + syngeneic ASCs; or (4) scaffold + allogeneic ASCs. Half of each cohort was harvested 4 or 8 weeks after surgery.

Spinal fusion was evaluated with radiography, microcomputed tomography, and light microscopy.

ASC Isolation and Cell Loading

All chemical reagents were obtained from Sigma-Aldrich (St. Louis, MO) or Fisher Scientific International, Inc. (Hampton, NH) unless otherwise indicated. Inguinal adipose tissue was harvested from 10-week-old male Fisher and ACI rats immediately following euthanasia by carbon monoxide asphyxiation. Isolation of ASCs was performed according to published methodologies.[25] Briefly, tissue was minced, washed, and suspended in an equal volume of phosphate-buffered saline containing 1% bovine serum albumin and 0.1% collagenase type I (Worthington Biochemical, Lakewood, NJ). Following a 60-min digestion at 37°C with agitation (50 rpm), the suspension was centrifuged at 1200 rpm for 5 min at room temperature to pellet cells from the stromal vascular fraction. The stromal vascular cells were plated at a density of 0.1 g of tissue digest per cm^2 in stromal media composed of Alpha Modified Eagles Medium (Gibco, Grand Island, NY) supplemented with 10% screened fetal bovine serum (Hyclone, Logan, UT) and1% antibiotic/antimycotic (Invitrogen, Carlsbad, CA). The cells were incubated for 3 to 6 days in a humidified 5% CO_2 incubator until they reached approximately 75% confluency, yielding about $25–30 \times 10^4$ cells/cm^2. At that time, the cells were passaged at a plating density of 5×10^3 cells/cm^2 and expanded to four or five passages. Cells were cryopreserved in aliquots of 7.5×10^6 cells/mL. The cryopreservation medium contained 90% fetal calf serum and 10% dimethyl sulfoxide (DMSO).[15] Cells were placed into a Nalgene Freezing Container (Nalgene, Rochester, NY) for 24 h at −80°C before transfer to liquid nitrogen.

Prior to surgery, cells were thawed and centrifuged at 1200 rpm for 5 min following addition of a 15:1 volume of stromal media to rinse the cells of cryopreservation media. Pelleted cells were resuspended in stromal media and loaded onto sterile, 7 × 5 × 2 mm β-tricalcium phosphate (80%)/type I bovine collagen blocks (20%) (Vitoss, Orthovita, Malvern, PA). The scaffolds are 88–92% porous, with pore diameters ranging from 1 to 1000 μm. Scaffolds were submerged in culturemedium for 5–10 mins, after which excess medium was withdrawn with a pipette. The cell suspension was slowly pipetted onto the scaffold using a 1000 μL pipetter to draw the suspension bidirectionally five times. Cells were loaded onto scaffolds at a concentration of 7500 cells/μL for a cell density of 3.75×10^6 cell/scaffold (53,571 cells/mm^3). They were allowed to adhere for 48 h in stromal medium before implantation.

Surgical Implantation

The rat posterolateral lumbar spinal fusion surgery was performed as previously described.[26] Briefly, male Fisher rats (Harlan Sprague-Dawley, Indianapolis, IN) were premedicated with a subcutaneous injection of 0.02 mg/kg glycopyrrolate (Robinul-V, Fort Dodge Animal Health, Fort Dodge, IA) and 0.5 mg/kg butorphanol (Torbugesic, Fort Dodge Animal Health). After 20 min, rats were administered isoflurane in an induction chamber to induce anesthesia. They were then maintained at 1.5% isoflurane via nose cone on a Bain circuit for the remainder of the procedure. The lumbar region was clipped and aseptically prepared with betadine and 70% isopropanol. A posterior midline skin incision was made over the lumbar spine. Two fascial incisions were made 3 mm lateral and parallel to the spinus processes. The L4 and L5 transverse processes were exposed using a combination of sharp and blunt dissection that was limited to the specific area of interest. A high-speed burr was used to decorticate the transverse processes bilaterally. The surgical sites were thoroughly lavaged with physiologic saline. Based on cohort assignment, scaffolds without cells or with syngeneic or allogeneic ASCs were placed on both sides of the spine such that they spanned between the midpoint of each transverse process. Just prior to placement, one corner of each scaffold was collected for scanning electron microscopic confirmation of cell loading. Animals in the no-treatment cohort underwent decortication

alone. Fascial and subcutaneous incisions were closed separately with 3-0 polyglactin 910 (Vicryl, Ethicon, Somerville, NJ) in a simple continuous pattern. To prevent migration, closure of the fascia around the implants effectively obliterated any potential space. Subcutaneous tissue was apposed similarly. Skin closure was achieved with tissue adhesive (Vetbond, 3 M, St. Paul, MN). Seven animals from each cohort were humanely euthanized by CO_2 asphyxiation 4 or 8 weeks after surgery.

Radiography

Anteroposterior and lateral spinal radiographs were performed postoperatively to confirm accurate scaffold placement and postmortem 4 or 8 weeks after implantation. Spines were evaluated for evidence of fusion by observers blinded to treatment, but the presence of the radio-opaque scaffold prevented accurate quantification of spinal fusion by standard scoring systems at the 4-week time point, a complication that has been previously described.[26] Radiographs were scored with the following system: 0 = no evidence of new bone formation; 1 = minimal bone formation without fusion; 2 = immature bone formation with questionable fusion; and 3 = solid bone with fusion likely. Each side of the spine was scored separately, and scores were combined for statistical analysis.

Scanning Electron Microscopy (SEM)

Cell loading onto the scaffolds was confirmed with SEM. Scaffold samples collected during surgery were fixed in 2% paraformaldahyde and 1.25% glutaraldehyde in 0.1 M sodium cacodylate (NaCaC) buffer, pH 7.4. Samples were rinsed in the same buffer and incubated with 1% osmium tetroxide in 0.1 M NaCaC. They were dehydrated in a series of ethanol-distilled water solutions, critical point dried from CO_2 in a Polaron bomb, and then sputter coated with gold and palladium. Samples were imaged with a scanning electron microscope (Quanta 200, FEI Company, Hillsboro, OR) at 15 kVP. The morphology of cells adhered to scaffold was objectively assessed in each sample.

Microcomputed Tomography

Spines were harvested immediately postmortem. Two-dimensional (2D) microcomputed tomography (μ-CT) imaging was performed by use of 0.04-mm slice widths with settings of 40 kV and 540 ms through a 180° rotation with imaging at 0.9° steps (SkyScan 1074, Skyscan n.v., Belgium). Two- (CTan, v 1.5.0.0) and three-dimensional (3D) (Mimics v 10.1, Materialise, Ann Arbor, MI) reconstructions were generated. Measurements on 2D and 3D images were performed with Mimics or CTan software packages, respectively. Total bone area (μm^2), bone perimeter (μm), and percent porosity (%) was measured on 2D slices at the level of the distal metaphysis of L4, the intervertebral space, and the proximal metaphysis of L5. For purposes of this study, metaphyses were considered to be at the midpoint of a line drawn between the closest intervertebral space and the middiaphysis of the vertebral body. The mean of the three slices was used for all statistical analyses. Total bony volume (mm^3) and surface area (mm^2) of the vertebral bodies, transverse processes, and fusion callus of L4 and L5 were measured on 3D images. Values were normalized to the anterior surface length of L5. Additionally, spinal fusion was quantified from the anterior aspect of each spine on 3D images by three independent observers blinded to treatment. The amount of bone between the transverse processes of L4 and L5 was evaluated using the radiographic fusion scoring system described above.

Histology

Spines were fixed in neutral-buffered 10% formalin and decalcified in citric-buffered formic acid. After decalcification, specimens were embedded in paraffin, and 5-μm-thick sections were stained with Masson's trichrome and H&E. The former stain produces high contrast

images with red bone, blue collagen, pink cell cytoplasm, and black cell nuclei.[27] Photomicrographs of each callus were generated with a digital camera (Model DFC 480, Leica Microsystems Inc., Bannockburn, IL) integrated into a light microscope (Model DM5000, Leica Microsystems Inc.) with polarizing capabilities. The midpoint of each callus was placed in the center of the field of view for all photomicrographs. The entire fusion mass was visible at a magnification of 5×. Bright-field images followed by polarized light images of sections stained with Masson's trichrome were captured. Next, a 40× bright-field photomicrograph of the center of the fusion mass was captured. The digital image data were exported as uncompressed tagged-image file format files and implemented in Adobe Photoshop v 7.0 (Adobe Systems Inc., Seattle, WA). Paired low magnification images were superimposed and the number of pixels corresponding to refractile tissue was quantified, divided by the total number of pixels in each image, and the quotient was multiplied by 100 to give a percentage. This procedure was performed to determine the percentage of lamellar bone in each sample. Due to parallel alignment of collagen fibers in lamellar bone versus woven bone or fibrous callus, polarized light is transmitted when the polarizers and lamellae are in the same plane, so lamellar bone is refractile when viewed with polarized light. The total number of inflammatory cells visible in each high magnification image was determined. Inflammatory cell infiltrate was distinguished based on standard phenotypic morphology and confirmed on H&E stained sections.[28]

Statistics

Treatment group comparisons for interval-scaled response variables were conducted using ANOVA models. The assumptions of normality and homoskedasticity were jointly assessed using the Breusch-Pagan/Cook-Weisberg test. For those variables for which the hypothesis of normality and homoskedasticity was rejected ($p<0.05$), the ANOVA-based tests used permutation methods to determine statistical significance. For each response variable, four a priori treatment group contrasts were tested. Adjustment for multiple testing was made using Sidak's method to control test size for each set of four contrasts at $\alpha = 0.05$. MANOVA was used to test the four treatment group contrasts for multivariate differences. Significance was considered at $p \leq 0.05$.

RESULTS

Animals

All rats tolerated the surgical procedure well and survived to the appropriate study end points without complications.

SEM

Cells were evident in all loaded scaffolds based on SEM imaging (Fig. 1). All cells evaluated had smooth surface contours and distinct points of attachment to the scaffold. There was no evidence of plasma membrane deformations or blebbing characteristic of cell demise.

Radiography

The presence of scaffold prevented accurate assessment of radiographic spinal fusion 4 weeks after implantation. This was due to the fact that remnants of scaffold were still visible 4 weeks after implantation based on direct comparisons of postoperative and 4-week postoperative radiographs. Although new bone was apparent at 4 weeks, it was difficult to quantify separately from scaffold, so it was not statistically analyzed in this study. Scaffold remnants were not detectable 8 weeks after implantation. Fusion scores in the allogeneic and syngeneic ASC scaffold cohorts were higher than the scaffold alone cohort 8 weeks after surgery, but the differences were not significantly different among the three cohorts (Table 1). Additionally,

callus was more mature based on a higher level of organization and less reactive bone in spines with ASC loaded scaffolds versus those with scaffold alone (Fig. 2). Overall, there was no effect of time or treatment on radiographic spinal fusion 8 weeks after implantation among scaffold treatment groups. There was no radiographic evidence of callus formation in the no treatment cohort throughout the study.

Microcomputed Tomography

2D CT—Bone area, perimeter, and percent porosity were significantly greater in the spines with scaffold versus those with no treatment regardless of the presence of ASCs at both time points. However, there was no effect of time or treatment among the scaffold treatment cohorts. Notably, bone area decreased or remained approximately the same in the allogeneic and syngeneic ASC cohorts, respectively, whereas it increased in the scaffold-only treatment group between the 4- and 8-week time points (Table 1). Bone perimeter increased in the scaffold-only treatment group, whereas it decreased in both the ASC treatment cohorts between 4 and 8 weeks. Finally, bone porosity increased in all three scaffold cohorts between 4 and 8 weeks, but the change was substantially higher in the scaffold-only treatment group versus the ASC treatment groups. Although these changes did not reach significance in this study, they are consistent with a more rapid remodeling process in the ASC loaded scaffolds.

3D CT—Normalized bone volume and area were significantly lower in the no-treatment cohort versus the scaffold treatment cohorts 4 and 8 weeks postimplantation; however, there was no effect of time or treatment among the scaffold treatment cohorts (Table 1). Bone volume decreased in both the allogeneic and syngeneic treatment groups between 4 and 8 weeks after implantation. It remained essentially the same in the scaffold only treatment group. Bone area decreased in all three treatment groups between time points, but least in the scaffold-only treatment group. These results are consistent with those described above.

Spinal Fusion—There were no effects of treatment on fusion scores among scaffold treatment cohorts with or without ASCs 8 weeks after implantation. Again, callus was more highly organized in the spines with ASC loaded scaffolds versus those with scaffold alone 8 weeks after implantation, consistent with a higher degree of remodeling (Fig. 3). Callus did not form in the no-treatment cohort during the study, and the presence of radio-opaque callus again complicated interpretation of fusion 4 weeks after implantation, so it was not statistically analyzed in this study.

Histology

There was poorly organized fibrous tissue with minimal inflammation between the L4 and L5 transverse processes in the no-treatment cohort at both time points. The fusion mass in all three groups was primarily fibrocartilagenous, with evidence of scaffold remnants 4 weeks after implantation, and there was no difference in refractile tissue percentage among scaffold treatment cohorts (Table 1). The fusion masses in the ASC treatment groups contained a significantly higher percentage of lamellar bone compared to the scaffold only treatment groups evidenced by a significantly greater percentage of refractile tissue in the tissue mass of the ASC treatment groups (Fig. 4). Four weeks after implantation, there was evidence of inflammation in all groups, but cell numbers were significantly higher in the scaffold only treatment group compared to both ASC treatment groups, which were not significantly different (Table 1). Inflammation was reduced 8 weeks after implantation compared to the 4-week time point, and there was no difference among scaffold treatment groups (Fig. 5).

DISCUSSION

Spinal fusion is an established treatment for degenerative and traumatic lumbar spine disorders.[2] Recently, patients treated with surgical stabilization for degenerative lumbar spondylolisthesis had better clinical outcomes than patients treated nonsurgically.[29] Mechanisms to accelerate the fusion process and obviate the need for bone grafting will decrease patient morbidity and contribute to improved outcomes. Implantation of ASCs may accomplish this clinical goal. In this investigation, syngeneic and allogeneic ASCs on a biocompatible scaffold resulted in superior callus maturation and remodeling 8 weeks after implantation compared to scaffold alone or no treatment in a rat model of lumbar fusion. Additionally, inflammatory cell infiltrate was significantly higher in spinal fusion masses with scaffold alone versus those with scaffolds and ASCs 4 weeks after implantation. The results of this study support continued investigation on the use of both allogeneic and syngeneic ASCs to facilitate and accelerate spinal fusion.

Adult BMSCs have been the focus of the majority of adult stem cell investigations to date[8,12] including their use to augment spinal fusion.[23,24] ASCs have received increased attention for tissue engineering purposes due to their equivalent phenotypic plasticity, greater abundance, and lower harvest morbidity relative to BMSCs.[8] Most investigations surrounding ASC osteogenic potential have been in vitro or subcutaneous implantation in vivo studies;[8,9,12,15,16,18,25] however, ASCs have been applied in animal models of long bone fracture and calvarial defect healing.[12,14] A recent study has demonstrated that porcine ASCs engineered to express bone morphogenetic protein 6 improved spinal fusion in an immunodeficient murine model.[17] The microenvironment regulates stem cell commitment toward specific lineages through intrinsic and extrinsic factors.[30] Due to complex interactions between stem cells and their environments, characterization of their behavior for specific applications is vital to optimizing their full therapeutic potential. The design of this study was based on this consideration as well as for comparative and translational purposes. The rat model of lumbar fusion is well established[26] and given the immunological characterization of rat strains, suitable for the evaluation of syngeneic and allogeneic ASC applications. Investigations in large animal spinal fusion models will be necessary to further characterize allogeneic and syngeneic behavior in vivo.

Quantity and quality of bone formation by transplanted stem cells relies in part on the carrier scaffold.[31] The ideal stem cell carrier differs between species and stem cell tissue of origin.[13,15,16,31] For this investigation, the bioabsorbable scaffold was selected based on current surgical applications and published information surrounding stem cell/scaffold interactions. The adherent ASCs on the scaffolds had normal morphology based on SEM imaging; however, precise quantification of viable cell numbers within each scaffold was not performed. Optimization of the loading mechanism for highly consistent stem cell loading will contribute to the benefits of this procedure, although this was beyond the purview of the current study.[16] Future studies will include compositional outcome measures and mRNA analyses to control for potential limitations imposed by the presence of the scaffold alone.

The ideal bone graft substitute for spinal fusion has osteoinductive, osteoconductive, and osteogenic capabilities inherent to native bone. The osteogenic quality has yet to be filled by traditional bone graft substitutes.[1,15] The current study reports accelerated fusion callus maturation in ASC treatment cohorts. Increases in 2D CT bone area and perimeter compared to maintenance or decreases in ASC treatment cohorts between 4 and 8 weeks are consistent with callus production in the scaffold group versus remodeling in the ASC groups. The 3DCTdata are consistent with the 2D data regarding the greatest decreases in bone volume and area in ASC cohorts. Evaluation of two CT image types allowed regional (2D) as well as whole structural (3D) outcome measures. The largest increases in 2D CT bone porosity in the scaffold

only treatment group reflects slower callus calcification following scaffold resorption as substantiated by bright-field and polarized light microscopy. Adult ASCs produce and ossify extracellular matrix in vitro and in vivo.[13,15,16,18] Osteocalcin and alkaline phosphatase mRNA and protein levels are increased in association with the osteoblastic induction and matrix mineralization process.[14] The ability of ASCs to assume an osteogenic phenotype obviates the cell recruitment and migration steps necessary for matrix production and mineralization, providing a temporal advantage over unloaded scaffolds. It is possible that higher cell loading densities, as well as preculture induction mechanisms will improve upon this advantage.[15,18,31] Future investigations will optimize these parameters based on information derived from the current study. Inclusion of earlier evaluation points may document further benefits of ASC implantation on spinal fusion.

It is promising that large callus volumes were not generated in this study. Unnecessary or exuberant callus can cause significant morbidity by impinging on and damaging surrounding tissues such as nerve, muscle, bone, and intervertebral disc.[32] Acceleration of spinal fusion without abundant callus may be illustrative of the inherent advantages of stem cells.

Both allogeneic and syngeneic ASCs were compared to investigate the feasibility of allogeneic ASC applications. There was significantly lower inflammatory cell infiltrate in the spinal fusion masses with ASC loaded scaffolds versus scaffold alone 4 weeks after implantation in this study. Lower numbers of inflammatory cells in cell-loaded scaffolds may be attributed to antiproliferative effects of ASCs on T cells[20,21] or possibly to localized high concentrations of SDF-1 produced by ASCs,[33] which have a repulsive effect on T cells. The initial inflammatory reaction observed in this study was likely directed against the scaffold which resolved with scaffold resorption as previously reported.[34] There was no difference in inflammatory infiltration between the two cell types in this study, consistent with immunosuppression by both allogeneic and syngeneic cells. The effect of ASC implantation on the systemic immune response in the spinal fusion model is the subject of a separate manuscript (submitted).

In conclusion, the results of this study support the benefits of ASC loaded scaffolds to facilitate spinal fusion. Reduced inflammation at an early time point and superior fusion mass mineralization and remodeling are clear advantages over scaffold alone. ASCs exhibit the benefits of bone marrow grafts without the associated morbidity or recognized potential for disease transmission. Additionally, use of “off the self” allogeneic cells will be advantageous in emergency situations or for patients with comorbidities or advanced age, reducing the availability of accessible adipose depots. Thus, the use of ASCs for spinal fusion as well as general bone regeneration merit further investigation as a therapeutic modality.

ACKNOWLEDGMENTS

This work was supported in part by funding from the Pennington Biomedical Research Foundation, the NIAMS (R41AR052542) (M.J.L., K.R.M., J.M.G.) and AR008523-05 (M.J.L.), and the CNRU Center Grant #1P30 DK072476 sponsored by NIDDK (G.Y., J.M.G.). The authors wish to acknowledge Dr. Xiying Wu, Sandra Robinson, and Olga Borkhsenious for technical assistance.

REFERENCES

1. Minamide A, Kawakami M, Hashizume H, et al. Evaluation of carriers of bone morphogenetic protein for spinal fusion. Spine 2001;26:933–939. [PubMed: 11317116]
2. Liao SS, Guan K, Cui FZ, et al. Lumbar spinal fusion with a mineralized collagen matrix and rhBMP-2 in a rabbit model. Spine 2003;28:1954–1960. [PubMed: 12973141]
3. Cui Q, Ming XZ, Balian G, et al. Comparison of lumbar spine fusion using mixed and cloned marrow cells. Spine 2001;26:2305–2310. [PubMed: 11679813]

4. Peterson B, Iglesias R, Zhang J, et al. Genetically modified human derived bone marrow cells for posterolateral lumbar spine fusion in athymic rats: beyond conventional autologous bone grafting. Spine 2005;30:283–289. [PubMed: 15682007]
5. Glassman SD, Carreon LY, Campbell MJ, et al. The perioperative cost of infuse bone graft in posterolateral lumbar spine fusion. Spine J 2008;8:443–448. [PubMed: 17526436]
6. Burkus JK, Schuler TC, Gornet MF, et al. Anterior lumbar interbody fusion for the management of chronic lower back pain: current strategies and concepts. Orthop Clin North Am 2004;35:25–32. [PubMed: 15062715]
7. Rao RD, Bagaria V, Gourab K, et al. Autograft containment in posterolateral spine fusion. Spine J 2008;8:563–569. [PubMed: 17923443]
8. Caplan AI. Adult mesenchymal stem cells for tissue engineering versus regenerative medicine. J Cell Physiol 2007;213:341–347. [PubMed: 17620285]
9. Im GI, Shin YW, Lee KB. Do adipose tissue-derived mesenchymal stem cells have the same osteogenic and chondrogenic potential as bone marrow-derived cells? Osteoarthritis Cartilage 2005;13:845–853. [PubMed: 16129630]
10. Klyushnenkova E, Mosca JD, Zernetkina V, et al. T cell responses to allogeneic human mesenchymal stem cells: immunogenicity, tolerance, and suppression. J Biomed Sci 2005;12:47–57. [PubMed: 15864738]
11. Niemeyer P, Kornacker M, Mehlhorn A, et al. Comparison of immunological properties of bone marrow stromal cells and adipose tissue-derived stem cells before and after osteogenic differentiation in vitro. Tissue Eng 2007;13:111–121. [PubMed: 17518585]
12. Knippenberg M, Helder MN, Doulabi BZ, et al. Adipose tissue-derived mesenchymal stem cells acquire bone cell-like responsiveness to fluid shear stress on osteogenic stimulation. Tissue Eng 2005;11:1780–1788. [PubMed: 16411823]
13. Cowan CM, Shi YY, Aalami OO, et al. Adipose-derived adult stromal cells heal critical-size mouse calvarial defects. Nat Biotechnol 2004;22:560–567. [PubMed: 15077117]
14. Gimble J, Guilak F. Adipose-derived adult stem cells: isolation, characterization, and differentiation potential. Cytotherapy 2003;5:362–369. [PubMed: 14578098]
15. Helder MN, Knippenberg M, Klein-Nulend J, et al. Stem cells from adipose tissue allow challenging new concepts for regenerative medicine. Tissue Eng 2007;13:1799–1808. [PubMed: 17518736]
16. Hicok KC, Du Laney TV, Zhou YS, et al. Human adipose-derived adult stem cells produce osteoid in vivo. Tissue Eng 2004;10:371–380. [PubMed: 15165454]
17. Sheyn D, Pelled G, Zilberman Y, et al. Nonvirally engineered porcine adipose tissue-derived stem cells: use in posterior spinal fusion. Stem Cells 2008;26:1056–1064. [PubMed: 18218819]
18. Yoon E, Dhar S, Chun DE, et al. In vivo osteogenic potential of human adipose-derived stem cells/poly lactide-co-glycolic acid constructs for bone regeneration in a rat criticalsized calvarial defect model. Tissue Eng 2007;13:619–627. [PubMed: 17518608]
19. Wrage PC, Tran T, To K, et al. The neuro-glial properties of adipose-derived adult stromal (ADAS) cells are not regulated by Notch 1 and are not derived from neural crest lineage. PLoS ONE 2008;3:e1453. [PubMed: 18197263]
20. McIntosh K, Zvonic S, Garrett S, et al. The immunogenicity of human adipose-derived cells: temporal changes in vitro. Stem Cells 2006;24:1246–1253. [PubMed: 16410391]
21. Yanez R, Lamana ML, Garcia-Castro J, et al. Adipose tissue-derived mesenchymal stem cells have in vivo immunosuppressive properties applicable for the control of the graft-versus-host disease. Stem Cells 2006;24:2582–2591. [PubMed: 16873762]
22. Lindholm TS, Ragni P, Lindholm TC. Response of bone marrow stroma cells to demineralized cortical bone matrix in experimental spinal fusion in rabbits. Clin Orthop Relat Res 1988;230:296–302. [PubMed: 3284680]
23. Minamide A, Yoshida M, Kawakami M, et al. The effects of bone morphogenetic protein and basic fibroblast growth factor on cultured mesenchymal stem cells for spine fusion. Spine 2007;32:1067–1071. [PubMed: 17471086]
24. Valdes M, Moore DC, Palumbo M, et al. rhBMP-6 stimulated osteoprogenitor cells enhance posterolateral spinal fusion in the New Zealand white rabbit. Spine J 2007;7:318–325. [PubMed: 17482115]

25. Aust L, Devlin B, Foster SJ, et al. Yield of human adipose-derived adult stem cells from liposuction aspirates. Cytotherapy 2004;6:7–14. [PubMed: 14985162]

26. Lu SS, Zhang X, Soo C, et al. The osteoinductive properties of Nell-1 in a rat spinal fusion model. Spine J 2007;7:50–60. [PubMed: 17197333]

27. Kim UK, Chung IK, Lee KH, et al. Bone regeneration in mandibular distraction osteogenesis combined with compression stimulation. J Oral Maxillofac Surg 2006;64:1498–1505. [PubMed: 16982308]

28. Badylak SF, Park K, Peppas N, et al. Marrow-derived cells populate scaffolds composed of xenogeneic extracellular matrix. Exp Hematol 2001;29:1310–1318. [PubMed: 11698127]

29. Weinstein JN, Lurie JD, Tosteson TD, et al. Surgical versus nonsurgical treatment for lumbar degenerative spondylolisthesis. N Engl J Med 2007;356:2257–2270. [PubMed: 17538085]

30. Djouad F, Delorme B, Maurice M, et al. Microenvironmental changes during differentiation of mesenchymal stem cells towards chondrocytes. Arthritis Res Ther 2007;9:R33. [PubMed: 17391539]

31. Mankani MH, Kuznetsov SA, Robey PG. Formation of hematopoietic territories and bone by transplanted human bone marrow stromal cells requires a critical cell density. Exp Hematol 2007;35:995–1004. [PubMed: 17960668]

32. Wong DA, Kumar A, Jatana S, et al. Neurologic impairment from ectopic bone in the lumbar canal: a potential complication of off-label PLIF/TLIF use of bone morphogenetic protein-2 (BMP-2). Spine J [E-pub ahead of print]. 2007

33. Sengenes C, Miranville A, Maumusx M, et al. Chemotaxis and differentiation of human adipose tissue CD34+/CD31− progenitor cells: role of stromal derived factor-1 released by adipose tissue capillary endothelial cells. Stem Cells 2007;25:2269–2276. [PubMed: 17525234]

34. Hing KA, Wilson LF, Buckland T. Comparative performance of three ceramic bone graft substitutes. Spine J 2007;7:475–490. [PubMed: 17630146]

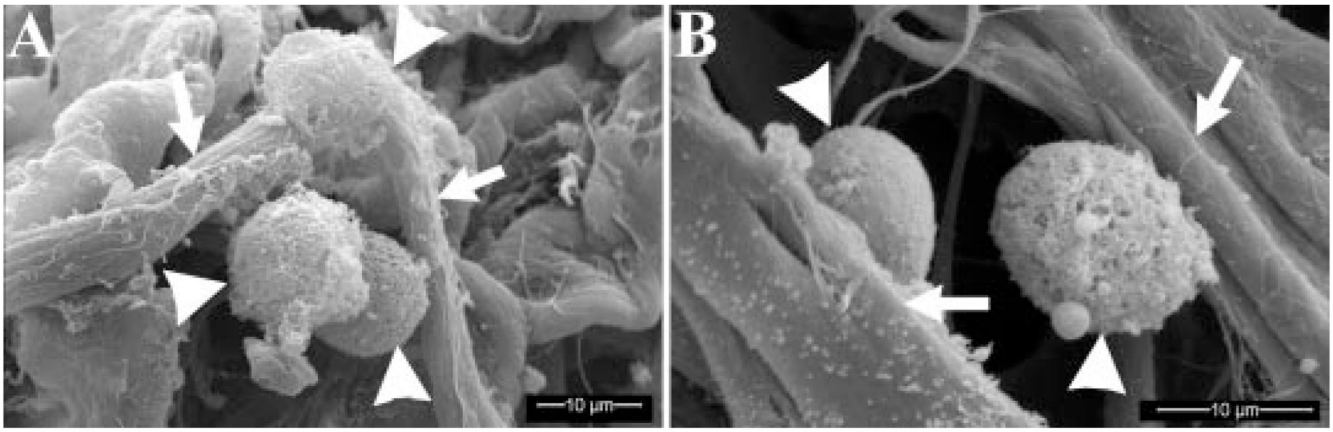

Figure 1.
Scanning electron photomicrographs of syngeneic (A) and allogeneic (B) ASCs (arrow heads) adhered to collagen fibrils (arrows) in the carrier scaffold just prior to implantation.

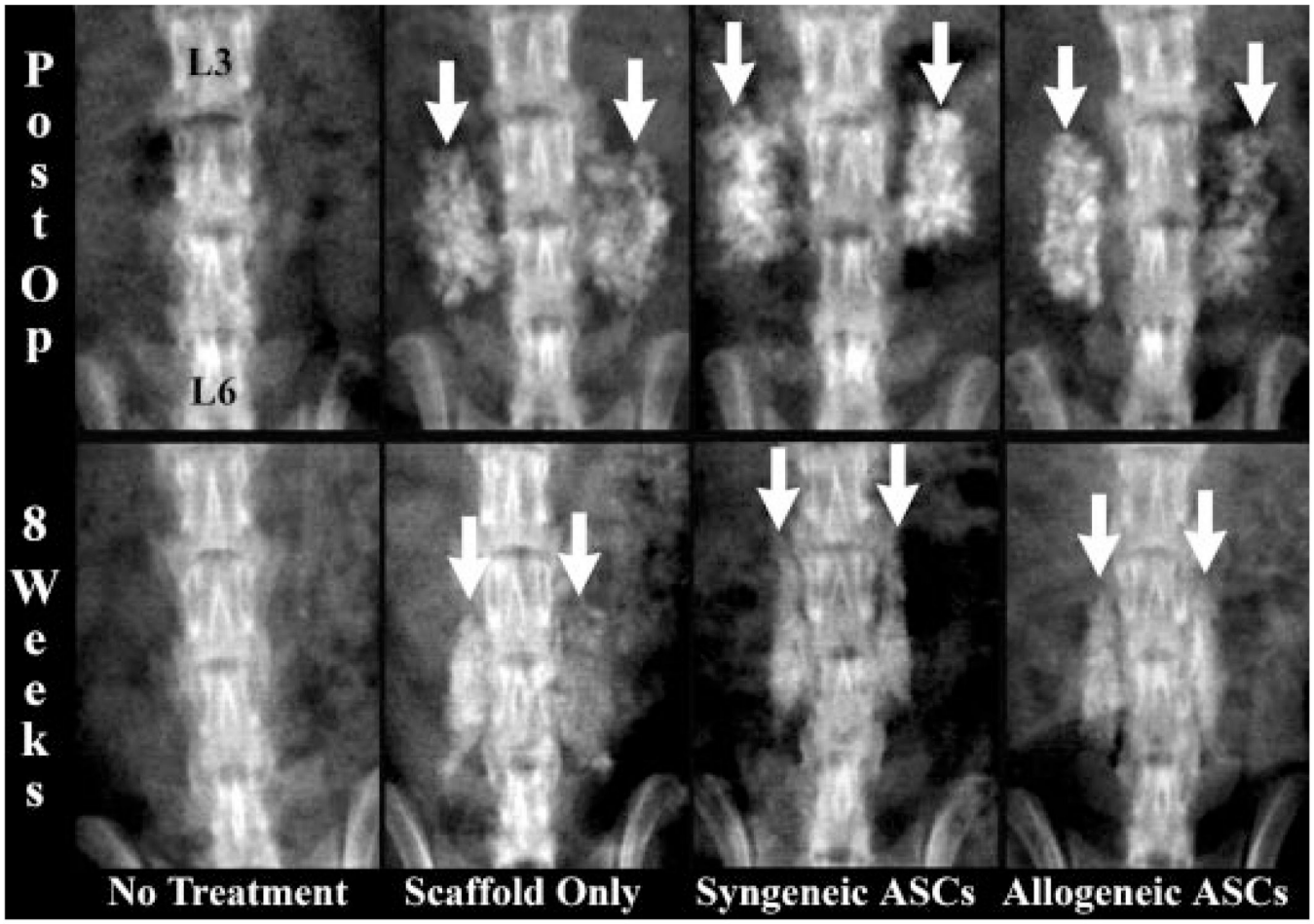

Figure 2.
Radiographs of the lumbar vertebra performed immediately (postop) and 8 weeks after implantation (8 weeks) of representative animals in each treatment cohort. The lumbar vertebra labeled in the first image are congruent with all images shown. The radioopaque scaffold is evident in the postop radiographs from scaffold treatment cohorts (white arrows). Callus is smaller, more organized, and less active in the ASC treatment cohorts 8 weeks after implantation (white arrows).

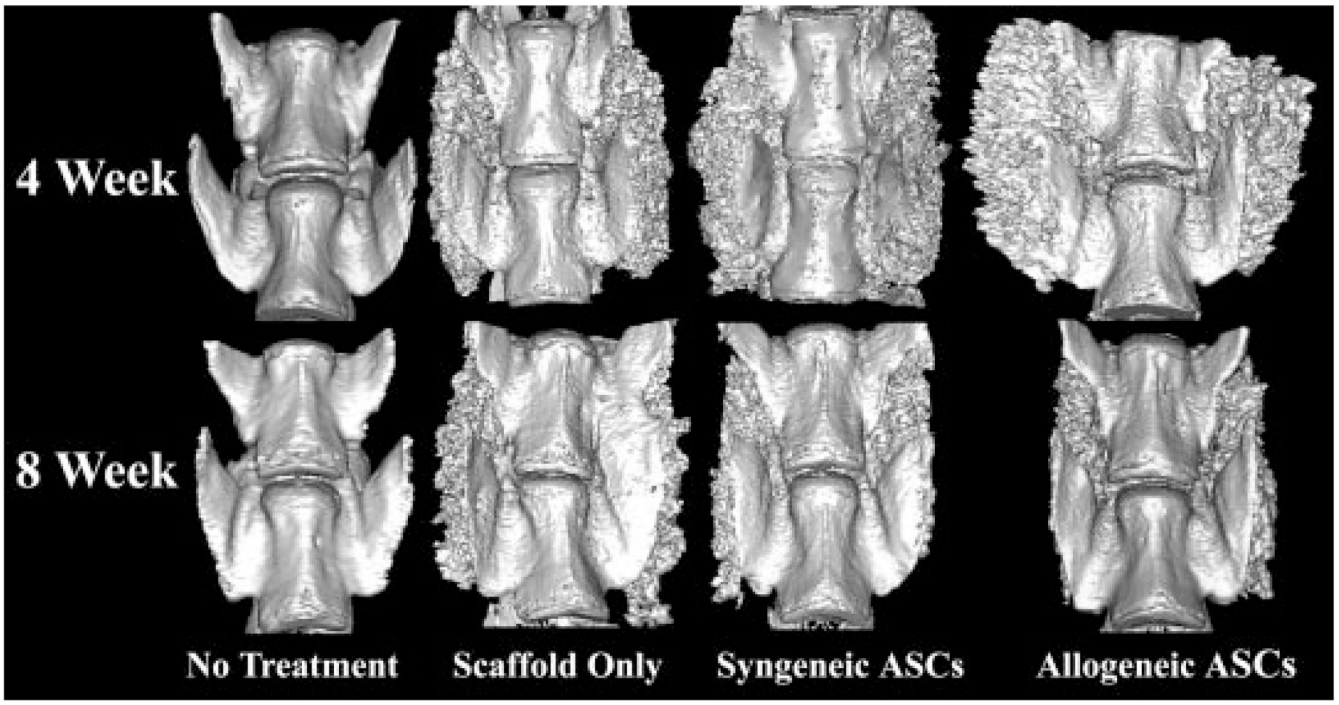

Figure 3.
Representative 3D reconstructions from μ-CT slices of the L4 (top) and L5 (bottom) vertebral bodies viewed from the anterior surface of the four treatment cohorts at each time point. Callus was more highly organized in the spines with ASC loaded scaffolds versus those with scaffold alone 8 weeks after implantation, consistent with a higher degree of remodeling.

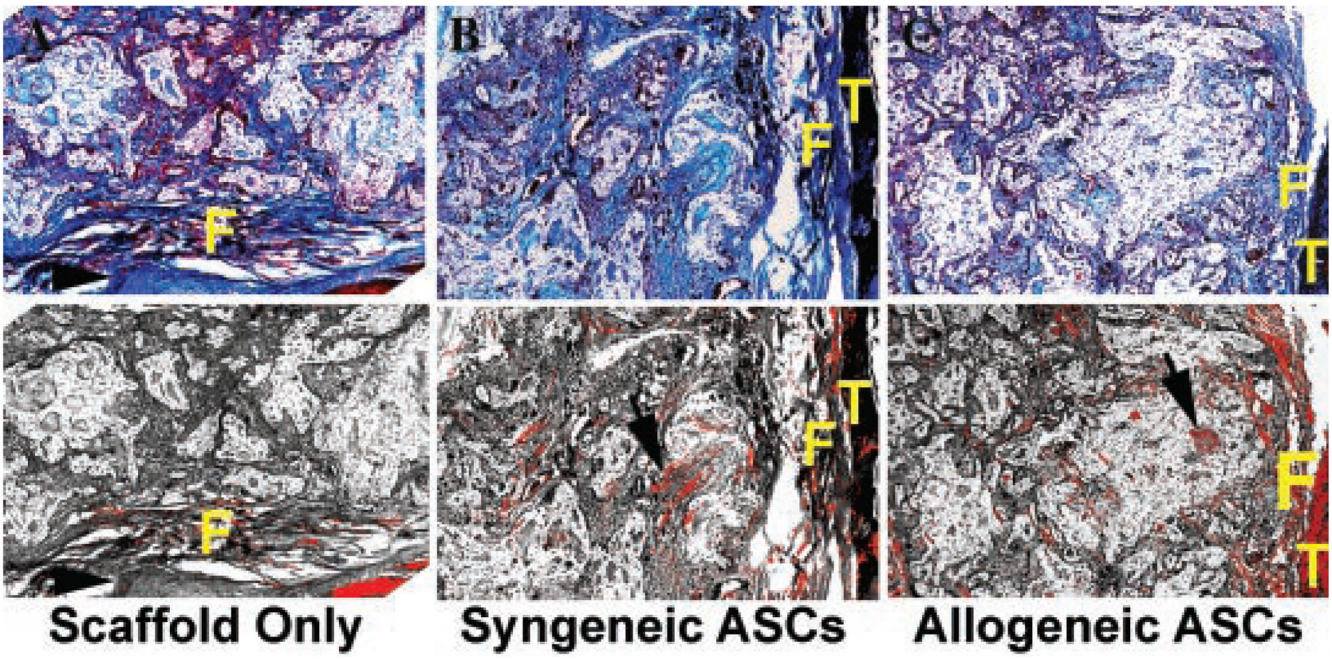

Figure 4.
Photomicrographs of representative fusion masses (5×) from ASC treatment cohorts 8 weeks after implantation. Bright-field images (upper) followed by polarized light images of sections stained with Masson's trichrome were captured. Paired images were superimposed for quantification of refractile tissue (black arrows) with graphics software (lower). Light diffraction due to tissue mineralization is pseudocolored red in composite images. Fibrous tissue (F) is visible in each image and transverse processes (T) are visible in two of the images. A vertebral body is apparent in the scaffold only image (arrow head).

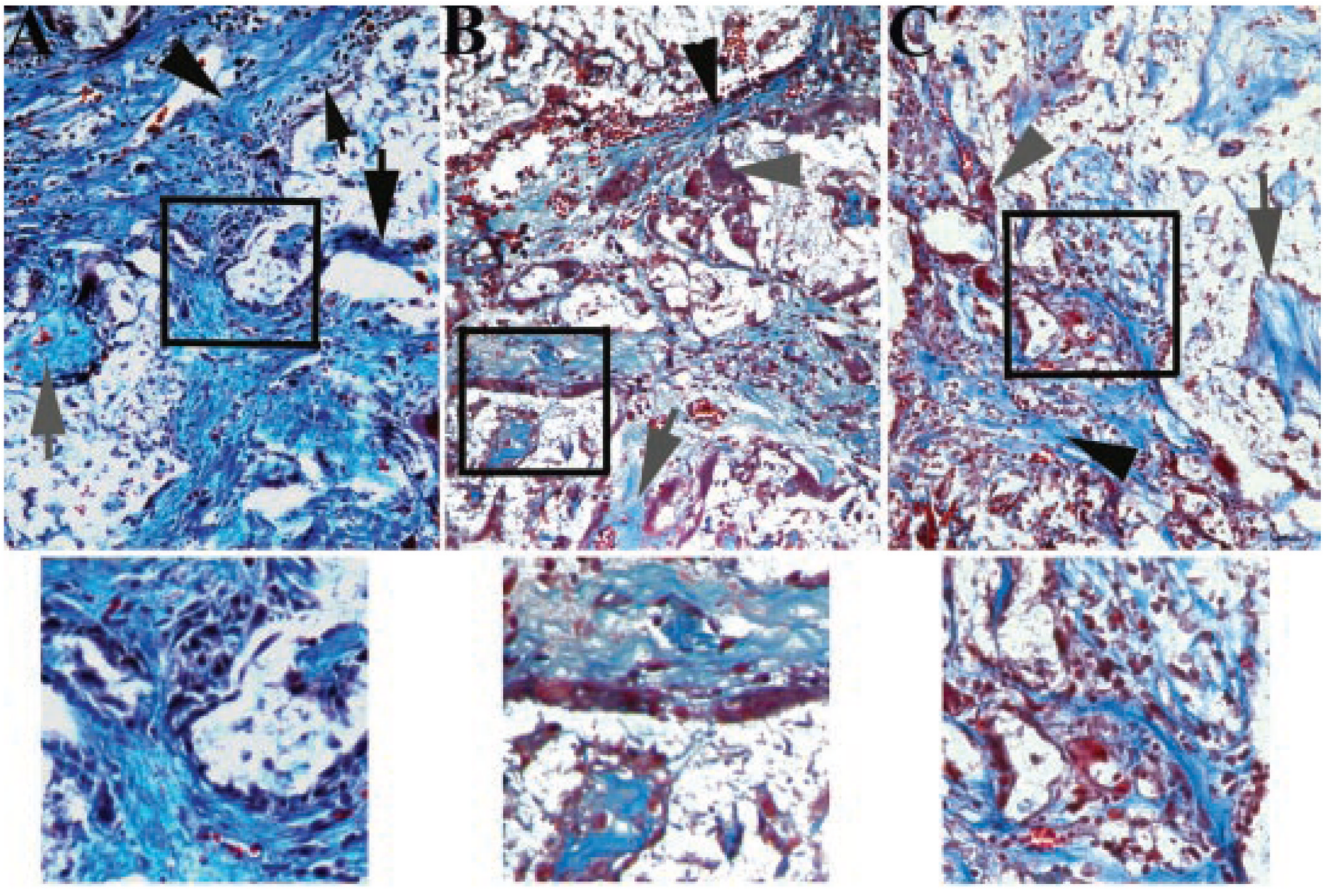

Figure 5.
Photomicrographs of the center of fusion masses (40×) from ASC treatment cohorts 4 weeks after implantation. Collagen fibers (black arrow head), scaffold remnants (large black arrow), woven bone (gray arrow), and amorphous matrix (gray arrow head) were evident in most images. Inflammatory infiltrate (small black arrow head) was significantly greater in the scaffold only treatment group (A) compared to the syngeneic (B) and allogeneic (C) ASC treatment groups that were not significantly different from one another. Higher magnifications of areas contained within black squares of each image illustrate the inflammatory infiltrate (A) and amorphous matrix (B and C) evident in the lower magnification images.

Table 1

Mean ± SEM of Radiographic, 2D Micro-CT, 3D Micro-CT, and Light Microscopy Outcome Measures Quantified in the Investigation

		Scaffold Only		Syngeneic ASCs		Allogeneic ASCs	
		4 Weeks	8 Weeks	4 Weeks	8 Weeks	4 Weeks	8 Weeks
Radiography	Fusion score	—	4.71 ± 0.15	—	4.95 ± 0.29	—	4.33 ± 0.29
2-D Micro-CT	Bone area (μm^2)	260 ± 28.9	309 ± 27.6	266 ± 29.2	267 ± 11.3	289 ± 11.1	244 ± 21.9
	Bone perimeter (μμm)	23.9 ± 2.55	24.9 ± 2.41	28.0 ± 2.27	22.9 ± 1.20	26.0 ± 0.75	20.3 ± 1.61
	Porosity (%)	11.8 ± 2.38	14.4 ± 1.78	13.0 ± 1.54	13.9 ± 1.03	12.8 ± 1.53	14.4 ± 1.55
3-D Micro-CT	Normalized bone volume (mm^2)	66.0 ± 1.96	64.1 ± 2.99	64.8 ± 5.46	60.2 ± 2.19	65.2 ± 3.36	57.0 ± 2.78
	Normalized bone area (mm)	259 ± 8.03	230 ± 7.59	259 ± 19.3	222 ± 9.66	258 ± 16.0	220 ± 12.6
	Fusion score	—	2.57 ± 0.17	—	2.50 ± 0.24	—	2.17 ± 0.32
Light	Refractile tissue (%)	0.23 ± 0.12	0.11^a ± 0.07	1.23 ± 0.48	0.77^b ± 0.09	1.45 ± 0.404	0.67^b ± 0.08
Microscopy	Inflammatory cells (#)	46.8^a ± 11.8	37.7 ± 23.7	18.3^b ± 0.85	33.5 ± 9.042	23.5^b ± 2.33	29.0 ± 5.99

Significant differences for given outcomes within time points are indicated with alphabetic superscripts. Values with different superscripts within a row are significantly different ($p < 0.05$).

J Orthop Res. Author manuscript; available in PMC 2009 September 1.